Desalination and Water Treatment
www.deswater.com

doi: 10.5004/dwt.2020.25401

185 (2020) 77–86
May

Experimental research and industrial application on bypass flue gas evaporation technology for FGD wastewater

Shuangchen Ma[a,b,*], Jin Chai[a,b], Xuan Bie[a,b], Kai Wu[a,b], Baozhong Qu[b], Wan Zhongcheng[c], Zhang Jingrui[c], Liu Ning[d], Yue Peiheng[d]

[a]*MOE Key Laboratory of Resources and Environmental Systems Optimization, Beijing 102206, China, Tel. +86-312-7525521; Fax: +86-312-7525521; emails: msc1225@163.com (S. Ma), 947793257@qq.com (J. Chai), 1162984974@qq.com (X. Bie), 495453835@qq.com (K. Wu)*

[b]*School of Environmental Science and Engineering, North China Electric Power University, Baoding 071003, China, Tel. +86-312-7522521; Fax: +86-312-7522521; email: 416734586@qq.com (B. Qu)*

[c]*Shengfa Environmental Protection Co., Xiamen, Fu Jian province 361000, China, Tel. +86-18959676828; email: 18959676828@163.com (W, Zhongcheng), Tel. +86-13696945075; email: 1049915084@qq.com (Z. Jingrui)*

[d]*Datang (Beijing) Water Engineering Technology Co. Ltd., Beijing 100097, China, Tel. +86-13696945075; emails: liuning@dteg.com.cn (L. ning), yueph@dteg.com.cn (Y. Peiheng)*

Received 11 April 2019; Accepted 24 December 2019

ABSTRACT

After the promulgation of the "water pollution control action plan" in China, zero liquid discharge (ZLD) of flue gas desulfurization (FGD) wastewater has become a hot spot for electric power conservation. In this paper, key factors affecting spray evaporation and optimum conditions were studied through laboratory experiments and industrial applications. The research results show that small atomized particle size, high flue gas flow rate, and high flue gas temperature were conducive to the complete evaporation, The optimum parameters through our lab test are listed as, flue gas temperature 300°C, the liquid flow rate 150 ml/min, the compressed air flow rate 15 L/min and the flue gas flow rate 300 m^3/h; What's more, industrial test was conducted in one specific power plant, the system can be safely run and the complete evaporation can be realized. The bypass flue has no adverse effects on subsequent equipment. This paper provides an optimized scheme for the FGD wastewater ZLD process and data to support achieving the FGD wastewater complete evaporation.

Keywords: FGD wastewater; Zero liquid discharge; High temperature; Flue gas evaporation

1. Introduction

Since the promulgation of the "Water Pollution Control Action Plan" in China [1], the flue gas desulfurization (FGD) wastewater with the problems of complex compositions and poor water quality has been widely concerned. As for desulfurization wastewater treatment, previous studies mainly focused on single pollutant removal and membrane purification to meet the discharge standard or reuse. Huang et al. [2,3] explored the removal performance of heavy metals in desulfurization wastewater using hybrid zero-valent iron, and the results showed that the removal efficiency of Se and Hg was more than 99%. Cui et al. [4] studied the electrolysis–electrodialysis process for removing chloride ion in wet FGD wastewater and the removal efficiency reached 83.3%. Na et al. [5] investigated the process feasibility of ultrafiltration-nanofiltration-reverse osmosis (UF-NF-RO) for treating

* Corresponding author.

desulfurization wastewater and producing the sulfuric acid and ammonium salt at the same time, the results showed in the process desulfurization wastewater could achieve the discharge standard and the by-production purity was high.

On June 9, 2017, the Ministry of Environmental Protection issued "Thermal Power Plant Pollution Prevention and Control Technology Policy" [6] and "Thermal Power Plant Pollution Prevention and Control of Feasible Technical Guidelines" [7] to regulate the emissions of wastewater, noise, solid waste and other pollutants from the power plants, which pointed out that water pollution should be controlled through rain and sewage diversion, reclaimed water reuse, and the combination of centralized and decentralized treatments; the FGD wastewater should be treated through neutralization, precipitation, flocculation, clarification, and other traditional processes, and FGD wastewater evaporation by waste heat, as well as crystallization using heat method and other treatment processes, was encouraged. Therefore, the zero liquid discharge (ZLD) of FGD wastewater is imminent.

The FGD wastewater is dried with hot steam in the commonly used technologies of evaporation and crystallization [8–10], but the system is complex with high investment and operation cost in present applications. The evaporation pond technology based on natural evaporation in some regions is simple and practical [11], but the efficiency is easily affected by season, temperature and other factors. The mechanical atomization evaporation technology has a large treatment capacity with low cost [12,13], but the salt pollution to the surrounding environment caused by wind loss is a serious problem that cannot be ignored. The wastewater is evaporated by flue gas waste heat in the traditional low-temperature flue evaporation technology [14,15], which works at 120°C–140°C after air preheater, with low investment and operating cost, but the evaporation efficiency is greatly influenced due to the low flue gas temperature by the fluctuation of boiler load. When the boiler load is low, the temperature of flue gas after air preheater may drop to 110°C or even lower, leading to incomplete evaporation. In addition, the wide application of ultra-low temperature electrostatic precipitators shortens the effective length of the flue duct, limiting the evaporation amount and reducing its efficiency. New ZLD technology for FGD wastewater, the bypass flue duct evaporation technology, was put forward in this paper, as shown in Fig. 1.

FGD wastewater was pumped to the airflow atomizer at the top of bypass flue and then atomized into droplets. The hot gas was extracted before air-preheater for drying. The atomized droplets are mixed with hot gas in the bypass flue; after mass transfer and heat transfer, the dry process was completed in a short time. The salt generated in the drying process was sent back to the main flue before electrostatic precipitator (ESP) with flue gas and then captured by ESP. The disadvantages of traditional flue evaporation technology mentioned above were overcome in the new technology effectively.

This paper analyzes the evaporation characteristics of bypass flue from laboratory experiments and field tests. The influences of the main parameters are explored. This study provides key data for the application of flue gas evaporation technology under high temperatures. The research results have important theoretical and practical values for the engineering practice of this technology.

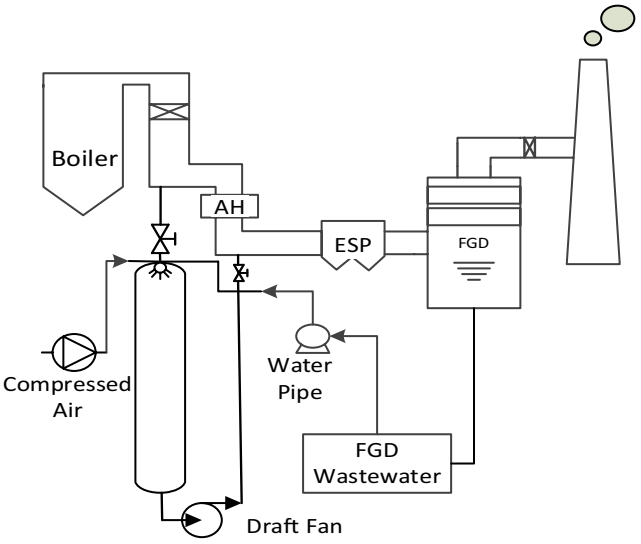

Fig. 1. Process of high-temperature bypass evaporation system.

2. Laboratory experiments

2.1. Experimental system

The experimental device of FGD wastewater evaporation is shown in Fig. 2. It consisted of two parts: flue gas heating and wastewater evaporation. First, the flue gas was introduced into the evaporator through the bypass fan, the flue gas was heated by heating tube, and the flue gas temperature was controlled by the temperature measuring device. When reaching the desired flue gas temperature, the FGD wastewater was atomized into small droplets through a two-fluid nozzle, and then fully contact with the high-temperature flue gas. Six temperature measurement points were set in the upper, middle and lower parts in the flue gas inlet, outlet and flue respectively. The maximum simulated flue gas flow rate was 350 m^3/h; the simulated flue gas temperature range was 100°C–400°C; the flow rate of FGD wastewater was up to 10 kg/L.

2.2. Determination of monitoring variables

2.2.1. Air characteristics [16,17]

The inlet air humidity in the experiment was obtained in the air enthalpy diagram at 20°C and 70% relative humidity. Each point in the figure indicates a certain nature and state of the humid air. As long as any two independent parameters are determined, another point can be determined.

$$\text{Absolute humidity } x = 0.622\frac{\phi p_s}{p - \phi p_s} \tag{1}$$

where ϕ represents relative humidity with the unit of %; p_s represents saturated vapor pressure with the unit of kPa; p represents standard atmospheric pressure with the value of 101.325 kPa.

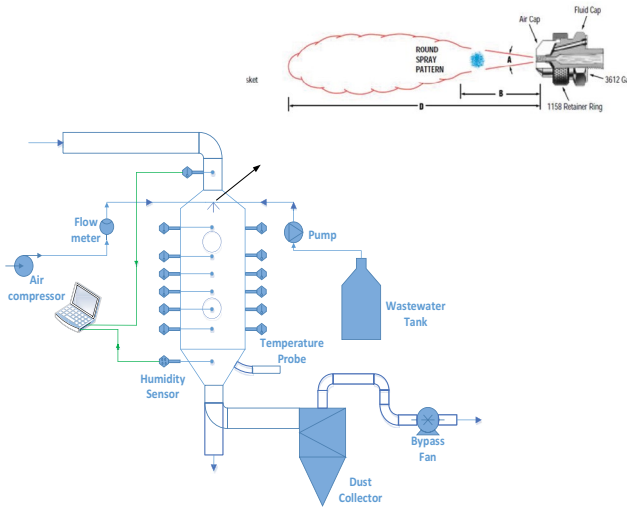

Fig. 2. Experimental system.

It is known that the saturated vapor pressure of air at 20°C is 2.3346 kPa, and the absolute humidity of the inlet air at this time is calculated as x_1 = 0.01 (kgH_2O/kg dry air). The temperature of the outlet air can be directly read to determine the key characteristics of the inlet and outlet air. The essential is to determine the slope of the line between the inlet and outlet air points represented in the *h*–*x* diagram.

$$K = c_w t_{m1} - \sum q \tag{2}$$

$$\sum q = q_m + q_L \tag{3}$$

When the solid content of FGD wastewater is small, the yield of the obtained product can be negligible, that is, $q_m = 0$.

Take the total heat transfer coefficient between the surface of the spray drying tower and the atmosphere K = 25kJ/(m² h°C). The heat dissipation surface area of the evaporator is:

$$A = \pi DH \approx \pi \times 0.2 \times 3 = 1.884 m^2 \tag{4}$$

Heat loss of when evaporating 1 kg wastewater is:

$$q_L = \frac{KA\left(t_2 - t_0\right)}{W} = \frac{47.1\left(t_2 - t_0\right)}{W} \tag{5}$$

Specific heat capacity of FGD wastewater is c_w = 4.186kJ/(kg°C), t_{m1} = 20°C, the slope can be calculated:

$$K = c_w t_{m1} - \sum q = 83.72 - \frac{47.1\left(t_2 - t_0\right)}{W} \tag{6}$$

where t_2 represents outlet temperature, °C; t_0 represents atmosphere temperature, °C.

Because the magnitude of the inlet and outlet air absolute humidity were 10^{-2}, the numerical fluctuations reflected in the enthalpy value were not obvious, that is, the process can be approximated as an equal enthalpy process. Thereby the actual outlet air absolute humidity x_2 can be obtained. If the water is completely evaporated under the condition of a certain amount of liquid M and the amount of inlet air Q, the water vapor generated by the partial evaporation of the water is completely transferred into the air before saturation, which is significant compared with the inlet air humidity. The increase of this part is converted into the absolute humidity to obtain the theoretical absolute humidity of the outlet air:

$$x_2 = x_1 + \frac{M}{Q} \tag{7}$$

where x_1 represents initial humidity of the air, 0.01 kg/kg; x_2 represents actual absolute humidity at the evaporator outlet, kg/kg.

2.2.2. Determination of complete evaporation

In order to facilitate data processing and judge the degree of evaporation, the concept of absolute humidity saturation is introduced.

$$\Delta = \frac{x_2}{x_s} \times 100\% \tag{8}$$

where x_s is absolute saturation humidity of outlet air that can be obtained from *h*–*x*, before the outlet air humidity reached saturation, the larger Δ was the higher degree of evaporation of wastewater. When the outlet air reaches saturation, Δ = 100%. The experiment is to find the point where Δ is exactly equal to 100%. It should be noted that the entire process must ensure that the outlet temperature is higher than the saturation temperature under the absolute humidity condition and that x_2 is less than the saturation humidity of the entire process. The calculation parameters are shown in Table 1.

There are two criteria to judge complete evaporation:

- If evaporated completely, the actual outlet air absolute humidity should be equal to the theoretical outlet absolute humidity. The simple criterion is that the evaporator outlet temperature is equal or slightly higher than the theoretical air absolute humidity when completely evaporated. The value of Δ can be used to judge the merits of the evaporation effect, the larger the Δ value is, the more beneficial to complete evaporation.
- If not completely evaporated, the simple criterion is that the outlet air temperature is much smaller than the theoretical air absolute humidity when it is completely evaporated. At this time, Δ = 100% is specified.

2.2.3. Temperature field

Twelve temperature probes were set up in the main evaporation area of the evaporator to measure the temperature field change in the evaporation area. The temperature change of the tower body can show the evaporation characteristics of FGD wastewater in different areas. The more the temperature drops, the more intense evaporation happens in this area. What's more, the other function of the probes was to observe the temperature drop in the main evaporation zone during the evaporation process. If the temperature drop was not obvious or even inversion of temperature occurs, it

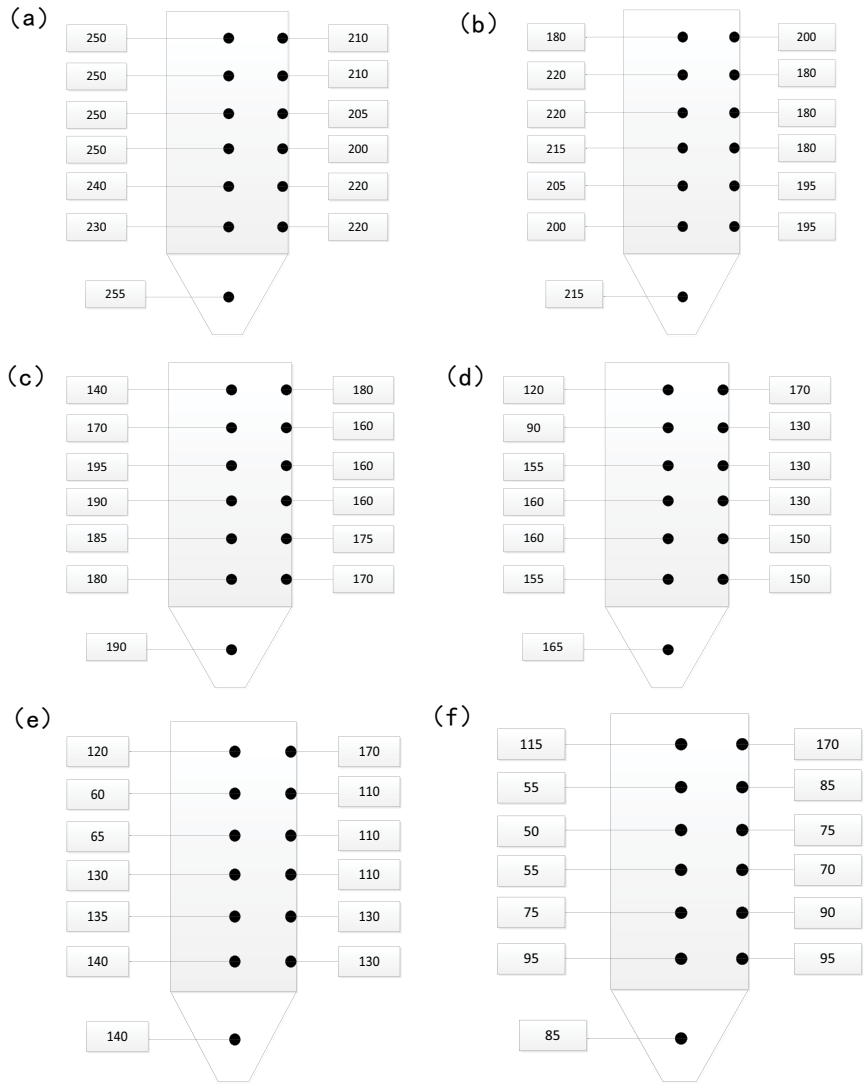

Fig. 3. Temperature field changing with the liquid flow rate. (a) 0, (b) 50, (c) 100, (d) 120, (e) 150, and (f) 180 ml/min.

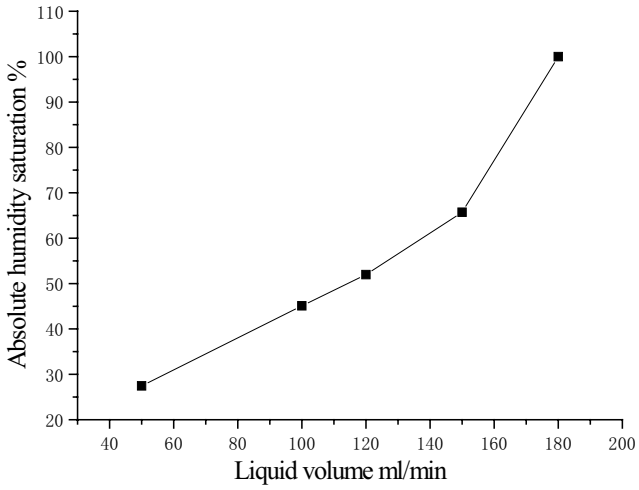

Fig. 4. Absolute humidity saturation changing with the liquid flow rate.

indicated that the droplets have been completely evaporated in the main evaporation zone.

2.3. Analysis of influencing factors

2.3.1. Liquid flow rate and gas–liquid ratio

When the flue gas temperature was 250°C, the flue gas flow rate was 250 m^3/h, the air compressor inlet was 15 LPM, and the liquid inlet range was 50–180 ml/min, the temperature field with the change of the liquid flow rate is shown as follows:

It can be seen from Fig. 3 that as the amount of liquid entering increases, the main evaporation zone moves down. According to the evaporator outlet temperature, Figs. 3a–e can be completely evaporated, while Fig. 3f cannot. The absolute humidity saturation changes with the amount of liquid entering are as shown in Fig. 4, it can be seen that as the amount of liquid increases, the humidity of the outlet air gradually increases until saturation. Under this working

condition, the maximum processing capacity of the evaporator will not exceed 180 ml/min.

2.3.2. Flue gas temperature

When the flue gas temperature range was 150°C–350°C, the flue gas flow rate was 300 m^3/h, the air compressor inlet was 15 LPM, the liquid inlet was 150 ml/min, the temperature field with the change of flue gas temperature was shown as follows:

It can be seen from Fig. 5 that as the temperature of the inlet flue gas increases, the main evaporation zone shows a significant upward trend, (a and b) cannot be completely evaporated according to the evaporator outlet temperature, while (c–f) can be completely evaporated; the absolute humidity saturation varies with the amount of liquid is shown in Fig. 6. It can be seen that as the temperature of the inlet flue gas increases, the humidity of the outlet air gradually increases until saturation, and the absolute humidity is saturated. The degree is gradually reduced, and it can be

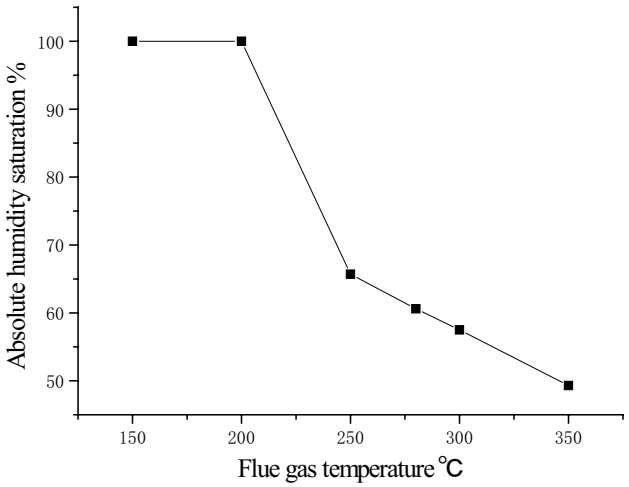

Fig. 6. Absolute humidity saturation changing with flue gas temperature.

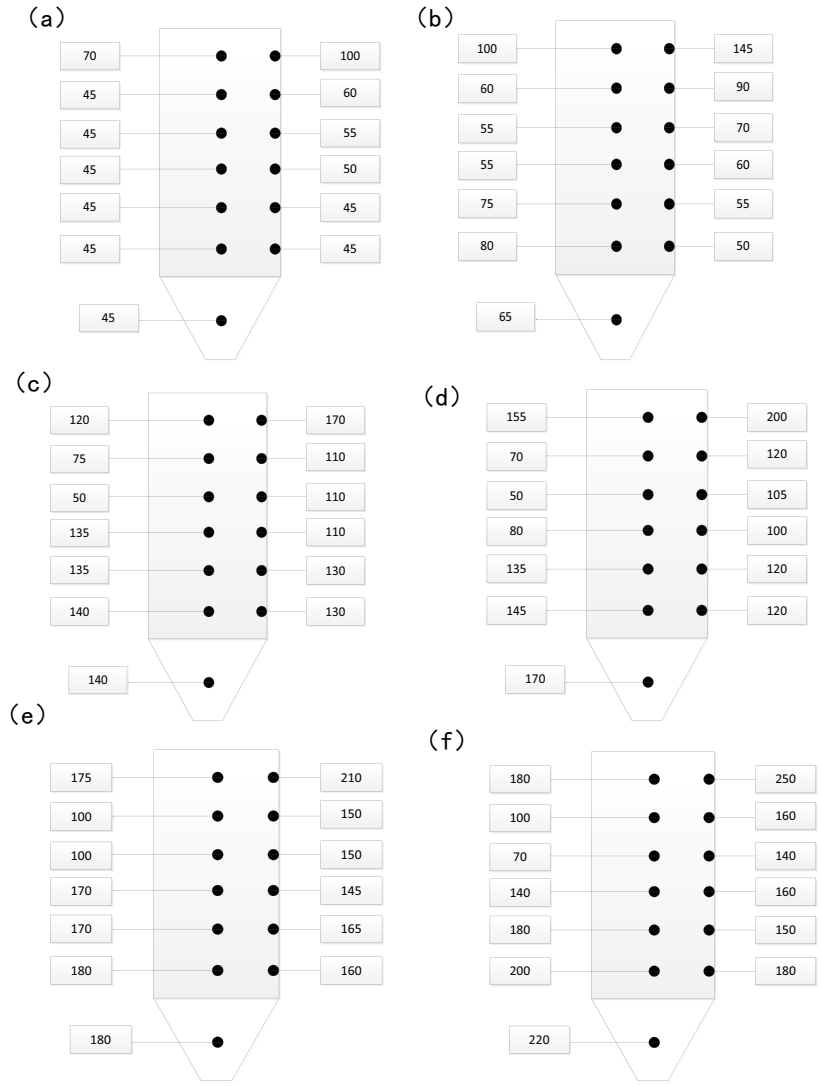

Fig. 5. Temperature field changing with flue gas temperature. (a) 150°C, (b) 200°C, (c) 250°C, (d) 280°C, (e) 300°C, and (f) 350°C.

explained that under this working condition, the inlet flue gas temperature should be higher than 200°C. At the same time, when the flue temperature reaches 250°C, the absolute humidity saturation decline trend is relatively slow, consider the energy-saving and operational safety of the system, the flue gas temperature should not exceed 300°C.

2.3.3. Flue gas flow rate

When the flue gas temperature was 250°C, the flue gas flow rate range was 150–350 m^3/h, the air compressor inlet was 15 LPM, the liquid inlet was 150 ml/min. The temperature field with the change of flue gas flow rate is shown as follows:

From Fig. 7, as the amount of imported flue gas increases, the main evaporation zone moves up, according to the evaporator outlet temperature, (a and b) cannot be evaporated, (c–e) can be completely evaporated; absolute humidity saturation with the change of the amount of liquid shown in Fig. 8, it can be seen that with the increase of the amount of imported flue gas, the absolute humidity saturation gradually decreases, the smaller the flue gas flow rate is, the lower the gas velocity is in the evaporator. The hot air with diminished ability carries droplets, which is not conducive to evaporation. Therefore, the flue gas flow should not be lower than 250 m^3/h. In addition, considering the excessive amount of flue gas extracted during the industrial application, the thermal efficiency of the boiler will decrease and the coal consumption will increase, the amount of extracted flue gas should not be too large.

2.4. Orthogonal experiment

To observe the interaction between the variables, compare the influence of each variable on the evaporation effect, and judge the optimal operating parameters under multi-factors conditions, "Four-factors and Four-levels" orthogonal experiment was designed. To make the data more

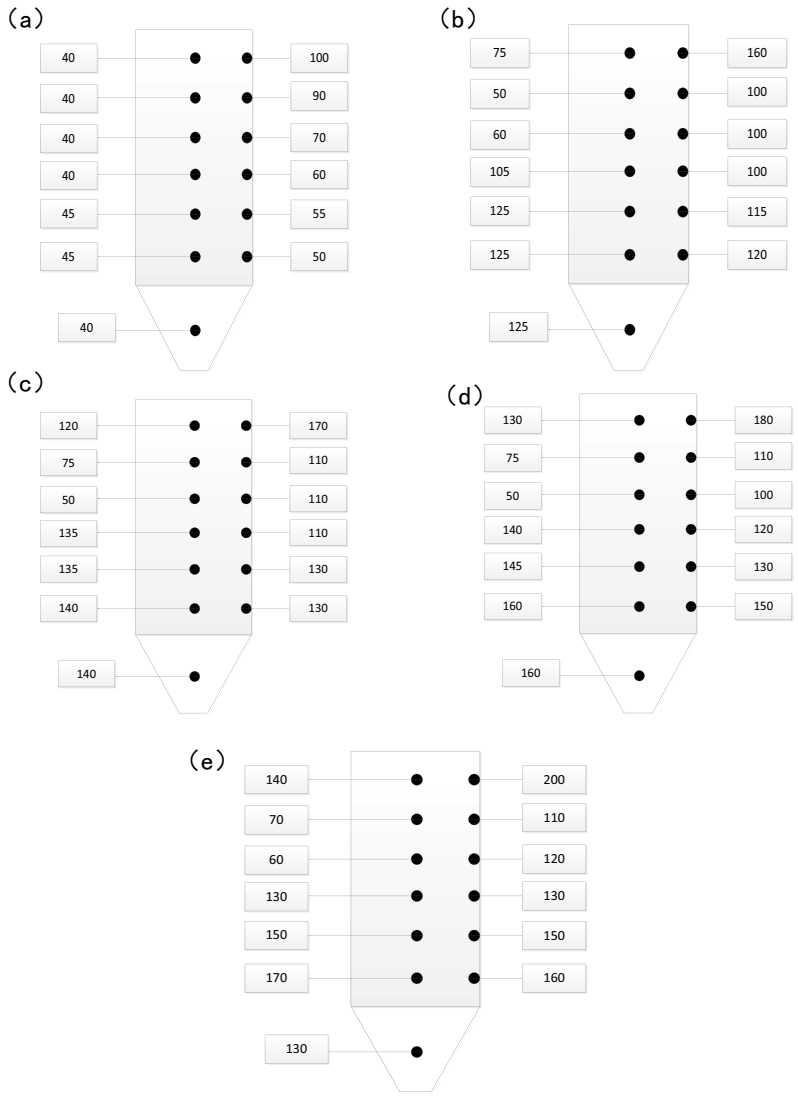

Fig. 7. Temperature field changing with flue gas flow rate. (a) 150, (b) 200, (c) 250, (d) 300, and (e) 350 m^3/h.

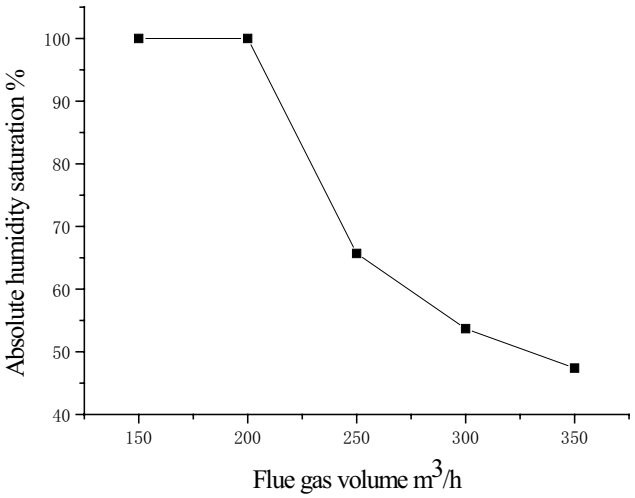

Fig. 8. Absolute humidity saturation changing with flue gas flow rate.

intuitive, Δ = 0 was specified in the incomplete evaporation state. The optimal conditions under multi-factor conditions were selected based on the value of Δ. The experimental parameters and results are shown in Table 2.

It can be concluded that the settings of the 13th and 15th are suitable parameters because the processing capacity of the 13th is small, the 15th group is the most suitable one. The optimum parameters were that flue gas temperature was 300°C, the liquid flow rate was 150 ml/min, the compressed air flow rate was 15 L/min and the flue gas flow rate was 300 m^3/h. The order of range is $R_1 > R_4 > R_2 > R_3$, which indicates that flue gas temperature is the greatest impact on the system, followed by liquid flow rate, the flue gas flow rate and compressed air flow rate.

3. Industrial test

3.1. Evaporator experiment

The industrial test was carried out in one 300 MW coal-fired power plant in Henan province, China, programmable

Table 1
Calculated parameters

Temperature	150°C	200°C	250°C	280°C	300°C	350°C
Saturated humidity	0.65	0.83	0.102	0.11	0.12	0.14
Flue gas density	0.83	0.74	0.67	0.635	0.61	0.565
Saturation temperature	30°C	35°C	40°C	45°C	50°C	55°C

Table 2
Conditions and results of the orthogonal experiment

	Flue gas temperature, °C	Flue gas flow rate, m^3/h	Compressed air flow rate, L/min	Liquid flow rate, ml/min	Δ
1	150	200	10	50	0
2	150	250	15	100	0
3	150	300	18	120	0
4	150	350	20	150	0
5	200	200	15	120	0
6	200	250	10	150	0
7	200	300	20	50	32.1
8	200	350	18	100	46.5
9	250	200	18	150	0
10	250	250	20	120	0
11	250	300	10	100	42.5
12	250	350	15	50	23.8
13	300	200	20	100	50
14	300	250	18	50	25
15	300	300	15	150	50
16	300	350	10	120	36.9
K_{ij}	0.000	12.500	19.850	20.225	
K_{ij}	19.650	6.250	18.450	34.750	
K_{ij}	16.575	31.150	17.875	9.225	
K_{ij}	40.475	26.800	20.525	12.500	
R_i	40.475	24.900	2.650	25.525	

logic controller was adopted by the bypass flue evaporation system to realize online remote monitoring of operating parameters and equipment conditions. Fig. 11 summarized the changes in various parameters during the bypass flue evaporation process. Temperature sensors were installed at the inlet, middle and outlet of the bypass flue respectively to monitor the temperature change, the evaporation effect can be initially determined. It can be seen from Fig. 9 that the evaporation of 0.9 t/h FGD wastewater requires a high-temperature gas flow rate of 9,000 Nm^3/h.

3.2. Impact of bypass flue evaporation system on power plant equipment

3.2.1. Effect of bypass flue evaporation on-air preheater

The bypass flue evaporation system uses the high-temperature flue gas before the air preheater and after the selective catalytic reduction to realize the evaporation of the reverse osmosis (RO) concentrated water. Under the premise that the heat exchange efficiency of the air preheater is constant, the heat amounts the primary air and the secondary air pass through the air preheater will decline. To this end, the impact of the process on the air preheater was analyzed and calculated. The results are as follows.

It can be seen from Table 3 that under the condition of boiler boiler maximum continuous rating, according to the design, 1 t/h FGD wastewater was evaporated, the proportion of flue gas extracted to the corresponding output of the boiler was 0.6189%, the air preheater outlet was compared with the primary and secondary air temperature decreased 0.4173°C. When 3.5 t/h FGD wastewater was evaporated, the proportion of flue gas extracted from the corresponding output of the boiler to produce total flue gas was 2.1654%, the air preheater outlet was compared with the primary and secondary air temperature decreased 1.5188°C. Under two operating conditions, the bypass flue evaporation process had less effect on the air preheater.

When the bypass flue evaporates concentrated water through RO, the temperature change of the air preheater before and after evaporation can be seen from Fig. 10. After bypass flue spray, there was almost no influence on the inlet and outlet flue temperature of the air preheater. The air preheater had a slight decrease in the secondary air temperature, but the fluctuation range was basically in the range before the spray. So the impact on the air preheater was small.

3.2.2. Effect of bypass flue evaporation on the FGD system

Fig. 11 shows the changes in the concentration of chloride and magnesium ions in the desulfurization tower before and after spraying (the concentrated water evaporation started on the 10th day). Due to the different displacement of FGD wastewater per day, at days 1–10 before the concentrated water spraying, the concentration of chloride ions in the desulfurization island was between 15,000 and 20,000 mg/L, and the concentration of magnesium ions was between 12,000 and 16,000 mg/L. After 10 d, the fluctuation range of the two ions was not much different from that before the spraying, so the bypass flue evaporation did not affect the ion balance of the desulfurization system.

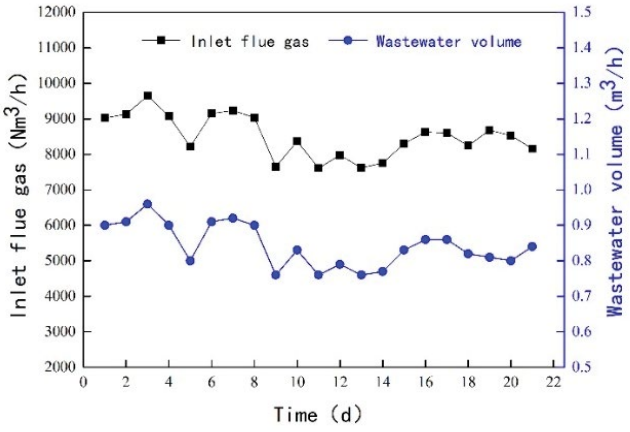

Fig. 9. Variation of flue gas flow rate and atomized water.

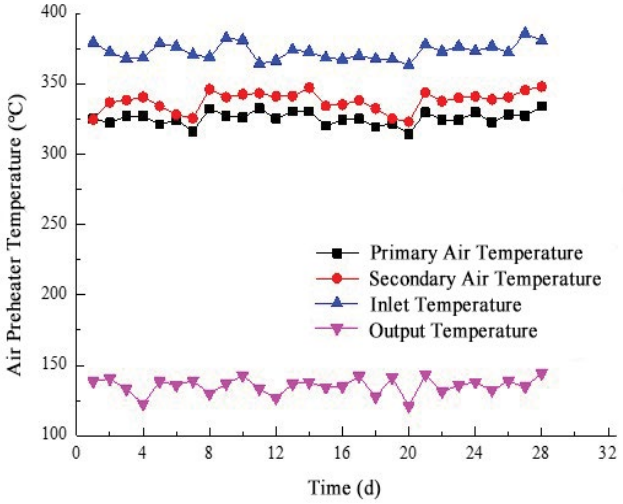

Fig. 10. Temperature variation of air preheater (the bypass flue evaporation beginning on the 10th day).

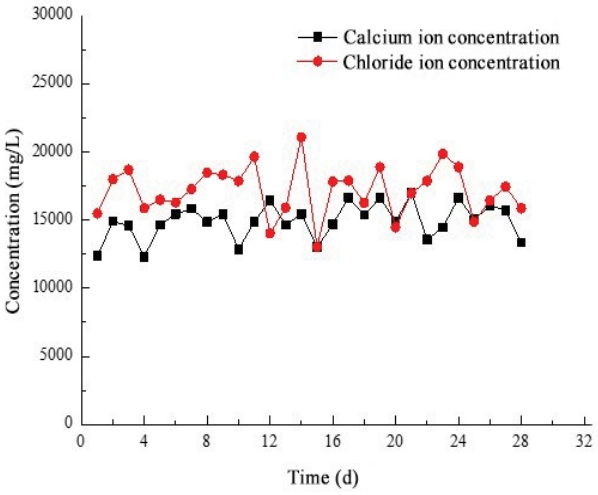

Fig. 11. The concentration of Cl^- and Mg^{2+} in FGD (the bypass flue evaporation beginning on the 10th day).

Table 3
Effect of bypass flue evaporation on-air preheater

Projects	Units	350 MW	
		100% BMCR	100% BMCR
Wastewater flow rate	t/h	1	3.5
Air preheater inlet/outlet flue gas temperature	°C	399/120	399/120
Extracted flue gas flow rate	m^3	6,522.0282	22,827.0987
Total flue gas flow rate	m^3	1,053,720.09	1,053,656.03
Proportion	%	0.6189	2.1665
Primary and second air temperature	°C	0.4173	1.5188

Table 4
Composition in the fly ash

No.	Projects	Standards	Before spraying	After spraying
1	Fineness	≤45%	41.4%	38.9%
2	Loss of burning	≤15%	6.39%	4.64%
3	Water content	≤1.0%	0.2%	0.1%
4	SO_3	≤3.0%	0.1%	0.08%
5	CaO	≤4%	0.08%	0.06%
6	Diazepam, mm	≤5	1.0	1.5
7	Chloride ion content	–	0.047%	0.103%

3.2.3. Effect of bypass flue evaporation on fly ash

After evaporation through bypass flue, the salt in RO concentrated water is captured by dust collector along with the dust in flue gas and finally enters into the fly ash. If the 2 × 350 MW unit's FGD wastewater flow rate was 150 ton/d and the chloride ion concentration is about 17,000 mg/L, the daily chloride ion production was 2.55 tons. Each boiler produced about 1,431,000 m^3/h flue gas; fly ash was about 30.23 ton/h, 2 sets of boilers produced 1,451.04 ton fly ash per day. Fly ash was mixed with cement as the raw material, the proportion of chloride ions in cement was 2.6/1,451.04 × 20% = 0.036%, which was lower than the national standard requirement 0.06% in silicate cement. Table 4 shows the composition of fly ash before and after spraying concentrated wastewater. It can be seen from the table that the chloride ion content in the fly ash increases to 0.103% after spraying wastewater. When the cement was blended at a ratio of 20%, the chloride ion proportion of cement was 0.103% × 20% = 0.0206%, which was lower than the theoretical calculation value of 0.036%. So, bypass flue evaporation did not affect the reutilization of fly ash.

4. Conclusions

The paper analyzed the evaporation characteristics of bypass flue from laboratory experiments and field tests. The influence of main parameters such as liquid flow rate, flue gas temperature and flue gas flow rate on the evaporation of FGD wastewater was explored. The most appropriate evaporation conditions were obtained and the operational stability and safety of the processing system at the field test stage were verified. The conclusions are shown as below:

- Liquid flow rate, flue gas temperature, and flue gas flow rate have a significant influence on the evaporation of FGD wastewater.
- Optimum parameters are listed as follows, flue gas temperature 300°C, the liquid flow rate 150 ml/min, the compressed air flow rate 15 L/min and the flue gas flow rate 300 m^3/h.
- Spray system can realize the safe running and complete evaporation. The bypass flue evaporation system has little effects on-air preheater and recycling utilization of fly ash.

Acknowledgment

The author is grateful to the Hebei key research and development plan (18273708D) for supporting this work.

Symbols

x	—	Absolute humidity
ϕ	—	Relative humidity, %
p	—	Atmospheric pressure, Kpa
K	—	Slope
c	—	Specific heat capacity
A	—	Area, m^2
D	—	Diameter, m
H	—	Height, m
t	—	Temperature, °C
M	—	Mount of liquid
Q	—	Mount of inlet air
q	—	Heat

Greek letters

s	—	Saturated
1	—	Inlet
2	—	Outlet
0	—	Atmosphere
w	—	Water
m	—	Product
l	—	Liquid

References

[1] Ministry of Environmental Protection of China, 2015. http://zfs.mep.gov.cn/fg/gwyw/201504/t20150416_299146.htm.

[2] Y.H. Huang, P.K. Peddi, C. Tang, H. Zeng, X. Teng, Hybrid zero-valent iron process for removing heavy metals and nitrate from flue-gas-desulfurization wastewater, Sep. Purif. Technol., 118 (2013) 690–698.

[3] Y.H. Huang, P.K. Peddi, H. Zeng, Pilot-scale demonstration of the hybrid zero-valent iron process for treating flue-gas-desulfurization wastewater: Part I, Water Sci. Technol., 67 (2013) 239–246.

[4] L. Cui, G. Li, Y. Li, Electrolysis-electrodialysis process for removing chloride ion in wet flue gas desulfurization wastewater (DW): influencing factors and energy consumption analysis, Chem. Eng. Res. Des., 1 (2017) 240–247.

[5] Y. Na, L. Fei, Z. Zhong, Integrated membrane process for the treatment of desulfurization wastewater, J. Ind. Eng. Chem. Res., 49 (2010) 3337–3341.

[6] Ministry of Environmental Protection of China, 2016. http://www.mep.gov.cn/gkml/hbb/bgth/201610/W020161009327656386426.pdf.

[7] Ministry of Environmental Protection of China, 2017. http://www.mep.gov.cn/gkml/hbb/bgg/201701/t20170117_394809.htm.

[8] US EPA, Technical Development Document for the Proposed Effluent Limitations Guidelines and Standards for the Steam Electric Power Generating Point Source, United States Environmental Protection Agency, US, 2013.

[9] C. Mosti, V. Cenci, ZLD Systems Applied to ENEL Coal-fired Power Plants, VGB Powertech, 1 (2012) 69–73.

[10] B. Pakzadeh, J. Wos, J. Renew, Flue Gas FGD Wastewater Treatment for Coal-fired Power Industry, Power Conference. American Society of Mechanical Engineers, America, 2014.

[11] S. Hoque, T. Alexander, P.L. Gurian, Innovative technologies increase evaporation pond efficiency, IDA J. Desal. Water Reuse, 2 (2010) 72–78.

[12] S.C. Ma, R. Gao, Research on Influencing Factors and Principles in the Process of Natural Evaporation for FGD Wastewater, Chinese Chemical Society Academic Annual Meeting, Beijing, China, 2016.

[13] D. Oates, P. Versteeg, E. Hittinger, Profitability of CCS with flue gas bypass and solvent storage, Int. J. Greenhouse Gas Control., 27 (2014) 279–288.

[14] S.C. Ma, J. Chai, G.D. Chen, Research on FGD wastewater evaporation: present and future perspectives, Renewable Sustainable Energy Rev., 58 (2016) 1143–1151.

[15] Shaw, Benefits of evaporating FGD purge water, Power, 152 (2008) 60–63.

[16] J.J. Bimbenet, P. Schuck, M. Roignant, Heat balance of a multistage spray-dryer: principles and example of application, Le. Lait., 82 (2002) 541–551.

[17] C.Y. Yu, B.H. Wang, X.Z. Wang, Spray Drying Technology, Chemical Industry Press, Beijing, China, 2013.